

Genetic Basis for Differential Activities of Fluconazole and Voriconazole against *Candida krusei*

Takashi Fukuoka,¹† Douglas A. Johnston,¹ Carol A. Winslow,² Marcel J. de Groot,² Catherine Burt,² Christopher A. Hitchcock,² and Scott G. Filler^{1,3*}

Division of Infectious Diseases, Department of Medicine, Harbor-UCLA Research and Education Institute, Torrance, California 90502¹; Pfizer Global Research and Development, Sandwich Laboratories, Sandwich, United Kingdom²; and UCLA School of Medicine, Los Angeles, California 90024³

Received 23 August 2002/Returned for modification 1 October 2002/Accepted 23 December 2002

Invasive infections caused by *Candida krusei* are a significant concern because this organism is intrinsically resistant to fluconazole. Voriconazole is more active than fluconazole against *C. krusei* in vitro. One mechanism of fluconazole resistance in *C. krusei* is diminished sensitivity of the target enzyme, cytochrome P450 sterol 14 α -demethylase (CYP51), to inhibition by this drug. We investigated the interactions of fluconazole and voriconazole with the CYP51s of *C. krusei* (ckCYP51) and fluconazole-susceptible *Candida albicans* (caCYP51). We found that voriconazole was a more potent inhibitor of both ckCYP51 and caCYP51 in cell extracts than was fluconazole. Also, the ckCYP51 was less sensitive to inhibition by both drugs than was caCYP51. These results were confirmed by expressing the CYP51 genes from *C. krusei* and *C. albicans* in *Saccharomyces cerevisiae* and determining the susceptibility of the transformants to voriconazole and fluconazole. We constructed homology models of the CYP51s of *C. albicans* and *C. krusei* based on the crystal structure of CYP51 from *Mycobacterium tuberculosis*. These models predicted that voriconazole is a more potent inhibitor of both caCYP51 and ckCYP51 than is fluconazole, because the extra methyl group of voriconazole results in a stronger hydrophobic interaction with the aromatic amino acids in the substrate binding site and more extensive filling of this site. Although there are multiple differences in the predicted amino acid sequence of caCYP51 and ckCYP51, the models of the two enzymes were quite similar and the mechanism for the relative resistance of ckCYP51 to the azoles was not apparent.

Candida krusei is an opportunistic pathogen that can cause serious infections in immunocompromised patients (1, 6, 7). This organism is intrinsically resistant to fluconazole. The new triazole voriconazole has greater in vitro activity than fluconazole against *C. krusei* (5, 15). Two mechanisms of azole resistance in *C. krusei* have been described. Isolates of *C. krusei* that are resistant to itraconazole exhibit reduced drug accumulation, suggesting that resistance to this drug is due to the activity of one or more drug efflux pumps (29). Recently, two ATP binding cassette transporters have been identified in *C. krusei*. Increased expression of these transporters is associated with reduced susceptibility to miconazole (9).

A second mechanism of azole resistance in *C. krusei* is diminished sensitivity of the target enzyme, cytochrome P450 sterol 14 α -demethylase (CYP51), to inhibition by an azole antifungal agent. We have determined previously that fluconazole resistance in some strains of *C. krusei* is mediated predominantly by this mechanism (17).

In the present study, we cloned the full-length *C. krusei* CYP51 and examined its contribution to the differential sensitivity of *C. krusei* to fluconazole and voriconazole. We also used computer-assisted molecular modeling to examine the

interactions of fluconazole and voriconazole with the predicted *Candida albicans* and *C. krusei* CYP51s.

MATERIALS AND METHODS

Organisms. *C. krusei* strains 91-1158, 91-1159, and 91-1161 are clinical isolates that were generously provided by Michael Rinaldi (San Antonio, Tex.). *C. albicans* SC5314 is also a clinical isolate and was kindly supplied by William Fonzi (Georgetown School of Medicine, Washington, D.C.). *Saccharomyces cerevisiae* AH22 (MAT α *leu2-3,2-112 his3-11,3-15 Can^r*) was a generous gift of Steven Kelly (University of Wales, Aberystwyth, United Kingdom) (10). *S. cerevisiae* TY310 (MAT α *pdrl pdr3::URA3 pdr5::TRP1 ade2-101 lys2-801 his3- Δ 200 leu2::PET56*) was a kind gift from Martine Raymond (Institut de Recherches Cliniques de Montreal, Montreal, Quebec, Canada) (27). *Escherichia coli* XL10-Gold (Stratagene, La Jolla, Calif.) was used for plasmid construction and amplification.

Ergosterol biosynthesis by cell extracts. The concentration of voriconazole required to inhibit by 50% (IC₅₀) the synthesis of ergosterol from [¹⁴C]mevalonic acid in cell extracts was determined exactly as described previously (17). Briefly, the organisms were grown overnight in Sabouraud dextrose broth at 37°C in a shaking incubator to an optical density at 600 nm of approximately 0.8. They were collected by centrifugation and then broken by vortexing with glass beads in 0.1 M potassium phosphate, pH 7.5, at a ratio of 4 g of beads to 1 g of organisms (wet weight). The resulting cell extract was separated from debris and unbroken cells by differential centrifugation. To measure sterol biosynthesis, 925 μ l of cell extract was added to 75 μ l of cofactor buffer (with or without voriconazole) to achieve the following final concentrations: 7 μ M glucose-6-phosphate, 5 μ M ATP, 3 μ M reduced glutathione, 2 μ M MnCl₂, 1 μ M NADP, 1 μ M NADPH, 1 μ M NAD, and 0.25 μ Ci of [¹⁴C]-mevalonic acid (10, 12). The samples were incubated at 37°C for 2 h and then saponified in ethanolic KOH at 80°C for 45 min. The sterols were extracted with petroleum ether (boiling point, 40 to 60°C), dried under nitrogen, and redissolved in chloroform. Next, they were separated by thin-layer chromatography on silica gel LK6D (Whatman Inc., Clifton, N.J.) using petroleum ether/diethyl ether (3:1, vol/vol) (23). The bands were visualized by iodine staining and the sterols were identified by comparison with commercially available standards, which were run in parallel. Finally, the sterol-contain-

* Corresponding author. Mailing address: Division of Infectious Diseases, Harbor-UCLA Research and Education Institute, Bldg. RB-2, 1124 West Carson St., Torrance, CA 90502. Phone: (310) 222-6426. Fax: (310) 782-2016. E-mail: sfiller@ucla.edu.

† Present address: Biological Research Laboratories, Sankyo, Co., Ltd., Shinagawa-ku, Tokyo 140-8710, Japan.

TABLE 1. PCR primers used in this study

Primer name	Sequence
Y572-01.....5'	ATGCCGTGGGTCGGCTCCGCCG 3'
Y572-02.....5'	CACCACAAAAGGTAAGTAAGGGG 3'
IPCR-1.....5'	GAGTGGTGAGATGGGTGTAAGCAT 3'
IPCR-2.....5'	GGTGTGCATCCCCTTACTTACCT 3'
CK14DM1.....5'	CGGGATCCTCTCTAGCAACAACAATGTCCG 3'
CK14DM2.....5'	CGGGATCCTTGATTGTGCGATTTTGGTTT 3'
CA14DM1.....5'	CGGGATCCAATATGGCTATTGTTGAAACT 3'
CA14DM2.....5'	CGGGATCCAACATACAAGTTTCTTTTTC 3'

ing bands were scraped from the plates, and their ^{14}C content was determined by liquid scintillation counting. All experiments were repeated at least three times using different batches of cell extracts.

Inverse PCR. Inverse PCR was used to amplify the 5' and 3' regions of the *ckCYP51* open reading frame (16, 28). We first amplified a fragment of *ckCYP51* from genomic DNA of *C. krusei* 91-1161 by PCR using primers Y572-01 and Y572-02 (Table 1). These primers were designed using the published incomplete *ckCYP51* sequence (GenBank accession number S75391) (4). This fragment was used to probe Southern blots of *C. krusei* genomic DNA to identify a restriction enzyme that was likely to cut outside of the open reading frame of *ckCYP51*. We determined that the *ckCYP51* probe hybridized with a 2.8-kb fragment of *C. krusei* DNA that had been digested with *Xba*I. Therefore, we digested *C. krusei* genomic DNA with *Xba*I and then isolated fragments of 2.5 to 3.5 kb in size by agarose gel electrophoresis. These fragments were ligated under dilute conditions to promote self-ligation. The self-ligated fragments were used as a template for inverse PCR using primers IPCR-1 and IPCR-2 (Table 1). The 1.8-kb product that was amplified was cloned into pGEM-T Easy (Promega Corp., Madison, Wis.) and sequenced.

Cloning of *ckCYP51* and *caCYP51* and heterologous expression in *S. cerevisiae*. The full-length *ckCYP51* and *caCYP51* were PCR amplified from genomic DNA of *C. krusei* and *C. albicans*, respectively. The high-fidelity *Pwo* DNA polymerase (Boehringer Mannheim) was used and the primers were CK14DM1 and CK14DM2 for *ckCYP51*, and CA14DM1 and CA14DM2 for *caCYP51* (Table 1). The *CYP51s* from the three strains of *C. krusei* and *C. albicans* SC5314 were first ligated into pGEM-T Easy for sequencing. Multiple independent clones were sequenced for each strain. Next, the *CYP51s* from *C. krusei* 91-1161 and *C. albicans* SC5314 were excised from their respective plasmids with *Bam*HI and ligated into pESC-LEU (Stratagene) to enable expression of the candidal *CYP51* in *S. cerevisiae* under control of the GAL1 promoter. In addition, PCR mutagenesis was used to change the CTG codons of *caCYP51* to TCT. This step was not necessary for *ckCYP51* because CTG encodes leucine in *C. krusei* (18). All mutations were confirmed by sequencing. The plasmids containing *ckCYP51* and *caCYP51* were transformed into *S. cerevisiae* AH22 and TY310 using the lithium acetate method (3). The transformants were grown on minimal medium (yeast nitrogen base without amino acids [Difco, Detroit, Mich.] with 2% glucose [wt/vol] and 2% agar [wt/vol]) supplemented with appropriate amino acids.

Susceptibility testing. The susceptibility of the *C. krusei* and *C. albicans* isolates to fluconazole and voriconazole was determined by the NCCLS M-27A broth microdilution method (14). Both fluconazole and voriconazole were dissolved in water. The fluconazole and voriconazole susceptibilities of the *S. cerevisiae* transformants were determined by the broth microdilution method of Sanglard et al. (22). The inoculum was 10^3 organisms, and the medium was yeast nitrogen base broth without amino acids containing 2% raffinose (wt/vol), 2% galactose (wt/vol), and histidine, adenine, and lysine (each at a concentration of 50 $\mu\text{g/ml}$). The incubation temperature was 30°C. Because of the slow growth of

the transformants, the endpoints were read at 3 days for strain AH22 and 6 days for strain TY310.

Construction of homology models of the CYP51s of *C. albicans* and *C. krusei*. Consensus homology models of *caCYP51* and *ckCYP51* were constructed using the program Modeller (version 3; Rockefeller University, New York, N.Y.) (21), as implemented in Quanta98 (version 98.1111; Molecular Simulations Inc., San Diego, Calif.). Initially four available bacterial crystal structures (CYP101, CYP102, CYP107A, and CYP108) were used to generate models of *caCYP51* (similar to the ones described by Ji et al. [8]) and *ckCYP51*. The bacterial P450s are considerably shorter in sequence than *caCYP51* and *ckCYP51*, making it very difficult to model the active site reliably. The publication of a crystal structure of CYP51 from *Mycobacterium tuberculosis* (mtCYP51 and 1ea1.pdb) (19) provided a better template for the construction of homology models. However, the structures of *ckCYP51* and *caCYP51* have an insertion just before the cysteine-binding pocket, and this insertion is not present in mtCYP51. The Protein Data Bank (2, 24) was searched for structures with a similar amino acid composition to the insertion, but none were obtained. Therefore, the area of this insertion could not be modeled reliably and limited conclusions about the structure of this area can be drawn.

A set of 20 models was produced. The best model was selected based on a PROCHECK (11) analysis of stereochemical quality and a visual inspection in Quanta98 to assess the location of the iron relative to the heme moiety, and the orientation of the amino acids involved in hydrogen bonds with the heme propionate moieties (e.g., R381 stabilizing the heme propionate moiety in *ckCYP51*).

Docking of inhibitors in the homology models for *caCYP51* and *ckCYP51*. Fluconazole was docked in the models of *caCYP51* and *ckCYP51* using the orientation derived from the crystal structure of mtCYP51 (1ea1.pdb) (19). The program Sybyl (Version 6.7; Tripos Inc., St. Louis, Mo.) was used to construct and energy minimize voriconazole and then superimpose it onto fluconazole in these models. The solvent accessible surfaces were generated using Quanta98.

Nucleotide sequence accession number of *ckCYP51*. The GenBank accession number of the *ckCYP51* sequence is AF531428.

RESULTS

Voriconazole is a more potent inhibitor of the *C. krusei* CYP51 than is fluconazole. We compared the susceptibilities of intact *C. krusei* and *C. albicans* cells to growth inhibition by fluconazole and voriconazole. As reported previously, all three strains of *C. krusei* exhibited decreased susceptibility to fluconazole, while *C. albicans* SC5314 was highly susceptible to this drug (Table 2) (17). Voriconazole was considerably more active than fluconazole against both species of *Candida* (Table 2). However, the MIC of voriconazole for the three isolates of *C. krusei* was 16-fold higher than its MIC for *C. albicans* (Table 2).

Next, we determined the concentrations of voriconazole and fluconazole required to cause a 50% inhibition in ergosterol synthesis by cell extracts of *C. krusei* and *C. albicans*. In these cell extracts, any effects of drug efflux pumps on azole susceptibility were obviated because the cell membranes were disrupted. Also, we have shown previously that the strains of *C. krusei* and *C. albicans* used in these experiments have similar amounts of CYP51 (17). Therefore, the experiments with the

TABLE 2. Concentrations of fluconazole and voriconazole required to inhibit the growth and CYP51s of *C. krusei* and *C. albicans*

Organism	MIC ($\mu\text{g/ml}$)		Mean IC_{50} ($\mu\text{g/ml}$) \pm SD	
	Fluconazole ^a	Voriconazole	Fluconazole ^a	Voriconazole
<i>C. krusei</i> 91-1161	32	0.5	0.243 \pm 0.130	0.014 \pm 0.004
<i>C. krusei</i> 91-1159	32	0.5	0.152 \pm 0.064	0.020 \pm 0.005
<i>C. krusei</i> 91-1158	64	0.5	0.230 \pm 0.118	0.020 \pm 0.005
<i>C. albicans</i> SC5314	1	0.031	0.010 \pm 0.002	0.0020 \pm 0.0006

^a Results are from our previous work (17).

TABLE 3. Antifungal susceptibilities of *S. cerevisiae* clones expressing *ckCYP51*, *caCYP51*, or the backbone vector

Gene or vector expressed	MIC ($\mu\text{g/ml}$)			
	<i>S. cerevisiae</i> AH22		<i>S. cerevisiae</i> TY310	
	Fluconazole	Voriconazole	Fluconazole	Voriconazole
<i>ckCYP51</i>	256	0.25	32	0.03
<i>caCYP51</i>	32	0.06	2	0.008
pESC-LEU	16	0.03	0.5	<0.004

krusei and *C. albicans* on the susceptibility of two different strains of *S. cerevisiae* to fluconazole and voriconazole. Strain AH22 was used because it has very low expression of its native *CYP51* (10). However, this strain had a relatively high fluconazole MIC, even when it was transformed with either *caCYP51* or the empty plasmid, pESC-LEU (Table 3). Therefore, we confirmed the results obtained with this strain by expressing *caCYP51* and *ckCYP51* in strain TY310, which does not express several drug efflux pumps and is highly susceptible to fluconazole (27). As predicted by our biochemical studies, the MIC of fluconazole for *S. cerevisiae* expressing *ckCYP51* was 8- to 16-fold higher than that of yeast expressing *caCYP51* (Table 3). Yeast strains expressing either *caCYP51* or *ckCYP51* were highly susceptible to voriconazole (Table 3). However, strains

expressing *ckCYP51* were fourfold less susceptible to voriconazole than were strains expression *caCYP51*.

Molecular modeling of the interactions of *caCYP51* and *ckCYP51* with fluconazole and voriconazole. To analyze the interactions of *caCYP51* and *ckCYP51* with fluconazole and voriconazole, homology models of these enzymes were constructed based on the crystal structure of *mtCYP51*, using the alignment shown in Fig. 1. The docking of fluconazole and voriconazole with *ckCYP51* and *caCYP51* was modeled as described in Materials and Methods. The predicted secondary structure of *ckCYP51* when it is bound by voriconazole is shown in Fig. 2. We compared the amino acids within an arbitrary 12-Å radius of theazole-binding site of *ckCYP51* and *caCYP51* to identify residues that are likely to mediate the differential binding of fluconazole and voriconazole to these enzymes. Our models suggest that the amino acids within 12 Å of the bound voriconazole or fluconazole are those from A122 to F134 and W145 to M148 in *ckCYP51* and A114 to F126 and S137 to K147 in *caCYP51* (Fig. 1 and 3). In models of both *caCYP51* and *ckCYP51*, the N1 of voriconazole and fluconazole interacts with the heme moiety, while two aromatic residues (Y126 and F134 in *ckCYP51*, and Y118 and F126 in *caCYP51*) mediate hydrophobic interactions with each drug. This hydrophobic interaction is predicted to be stronger with voriconazole than it is for fluconazole, due to the extra methyl

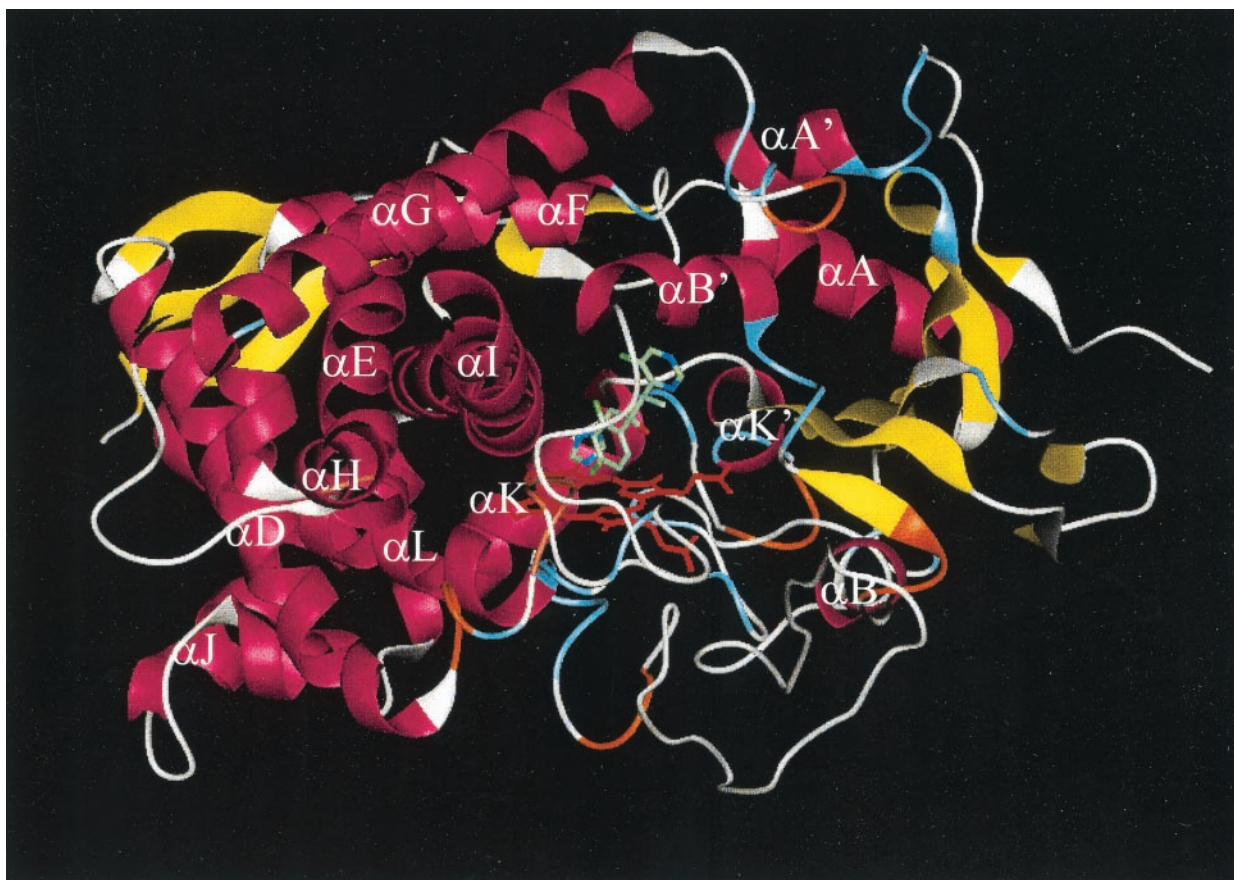


FIG. 2. Secondary structure of *ckCYP51* docked with voriconazole. At this level of detail, *caCYP51* and *ckCYP51* are identical, as the side-chains are not shown. α -Helices are shown in purple, β -sheets are shown in yellow, three-turns are shown in aqua, four-turns are shown in orange, the heme moiety is shown in red, and regions with no secondary structure are shown in white. Voriconazole is shown in green.

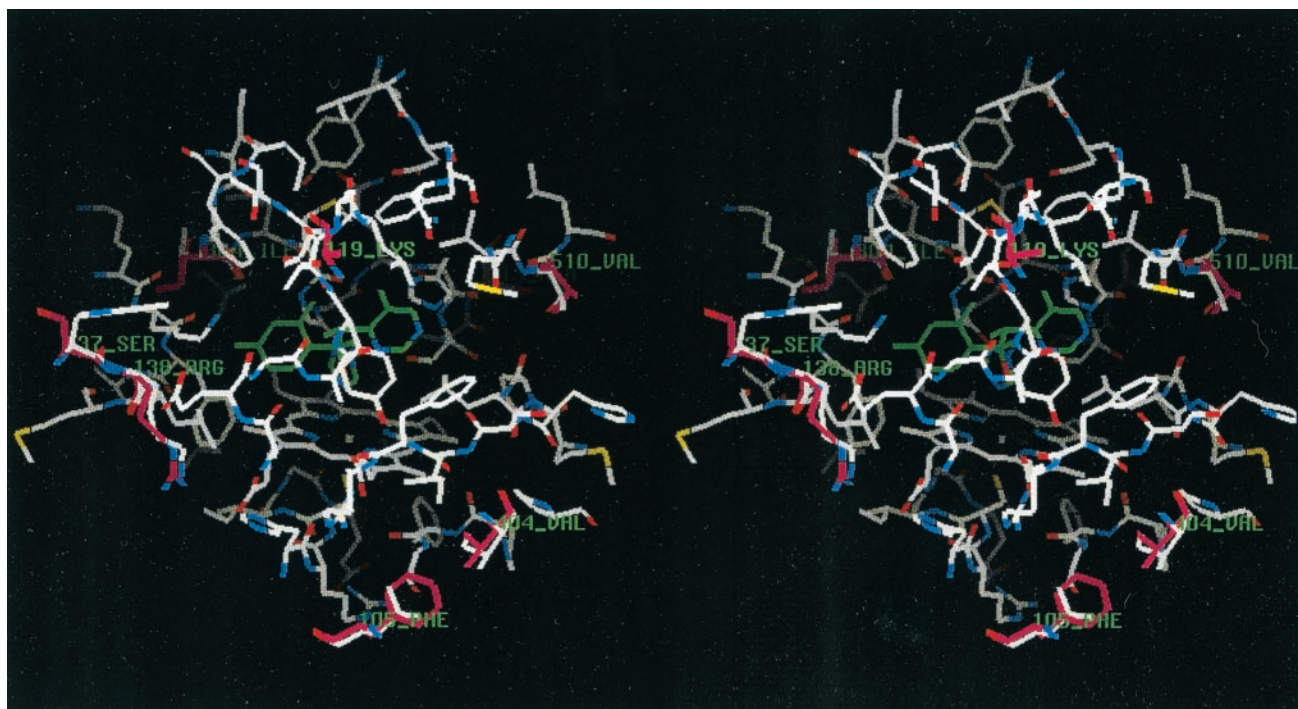


FIG. 3. Stereo display of active site region of ckCYP51 within 12 Å of voriconazole. The carbon atoms of voriconazole are shown in green. Amino acid side chains that are different in caCYP51 are shown with purple carbon atoms and are labeled (see also Table 4 and Fig. 1).

group on voriconazole. As a result, voriconazole fills the available space in the active site more extensively than does fluconazole (Fig. 4), explaining why voriconazole is a more potent inhibitor of both caCYP51 and ckCYP51 than is fluconazole.

The amino acids that are within 12 Å of the bound drug and that differ between ckCYP51 and caCYP51 are listed in Table 4 and shown in Fig. 3. None of these amino acids are predicted to interact with either voriconazole or fluconazole through their side chains. The amino acids that are the most different in the two CYP51s, K119 versus T127 and S137 versus W145 (caCYP51 versus ckCYP51), are not orientated towards the active site. Therefore, the present model does not provide a clear explanation for the reduced sensitivity of ckCYP51 to both drugs.

DISCUSSION

Previous biochemical studies had indicated that fluconazole resistance in some strains of *C. krusei* occurs because the ckCYP51 is resistant to inhibition by this drug (17). This conclusion is supported by our present findings that *S. cerevisiae* strains that express ckCYP51 are significantly less susceptible to fluconazole than are strains that express caCYP51. We also found that voriconazole was considerably more active than fluconazole in inhibiting the growth of *C. krusei* in vitro. These results are consistent with those of other investigations (5, 15). Both the biochemical and gene overexpression studies demonstrated that the increased antifungal activity of voriconazole is due in part to the enhanced ability of this drug to inhibit ckCYP51.

We found that voriconazole was 64- to 128-fold more active

than fluconazole at inhibiting the growth of *C. krusei*, whereas in the experiments with cell extracts, voriconazole was only 8- to 17-fold more potent than fluconazole in inhibiting ckCYP51. Therefore, an additional factor other than the enhanced inhibition of ckCYP51 must contribute to the increased activity of voriconazole against *C. krusei*. This additional factor may be the ability of voriconazole to achieve a high intracellular concentration within the fungal cell. At present, it is not possible to directly compare the intracellular accumulation of fluconazole and voriconazole because radiolabeled voriconazole is not available.

The activity of drug efflux pumps significantly influences intracellular accumulation of azoles and contributes to antifungal resistance in some isolates of *C. krusei* (9, 29). Thus, it is possible that voriconazole is poorer substrate for such pumps than is fluconazole. However, using radiolabeled fluconazole, we have previously determined that the fluconazole uptake of the three strains of *C. krusei* used in the present study was similar to that of *C. albicans* SC5314, which is susceptible to fluconazole (17). Thus, these strains of *C. krusei* do not appear to have high-level expression of azole efflux pumps.

We used computer-assisted homology modeling to compare the predicted structures of ckCYP51 and caCYP51, and to determine the structural basis for the differences in activity of fluconazole and voriconazole against ckCYP51 and caCYP51. Several models have been derived for caCYP51 previously, and these different models yield different predictions about how fluconazole interacts with caCYP51 (8, 25, 26). Our models of caCYP51 and ckCYP51 agree with the one developed by Talele and Kulkarni (26). In this model, the N-1 atom of fluconazole (or voriconazole) interacts with the heme moiety

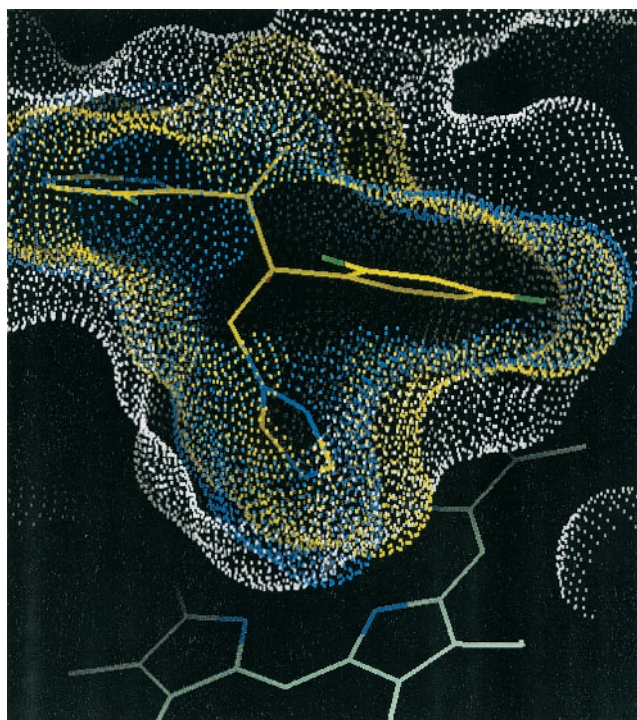


FIG. 4. Solvent-accessible surface of the ckCYP51 active site (white) with the surfaces of fluconazole (blue) and voriconazole (yellow). Voriconazole (shown with yellow carbon atoms) fills more of the available space in the active site than does fluconazole. The “pocket” highlighted is formed mainly by the side chains of Y126 and F134 (corresponding to Y118 and F126 in caCYP51) and the backbone of T130 (T122 in caCYP51). The heme moiety is shown as the green stick figure at the bottom of the figure to indicate the orientation.

as well as Y118 and F126 of caCYP51. In ckCYP51, the two aromatic amino acids that are predicted to interact with fluconazole are Y126 and F134. Our analysis predicts that voriconazole is a more potent inhibitor of both caCYP51 and ckCYP51 than is fluconazole because the extra methyl group of voriconazole results in a stronger hydrophobic interaction with these aromatic amino acids and more extensive filling of the substrate binding site.

Although some of the amino acids that were within 12 Å of the active site differed between caCYP51 and ckCYP51, none of these amino acids were predicted to interact with voriconazole or fluconazole through their side chains. Therefore, our models of caCYP51 and ckCYP51 do not provide a clear

TABLE 4. Differences between caCYP51 and ckCYP51 within 12-Å radius from active site^a

caCYP51	ckCYP51	Difference (caCYP51 → ckCYP51)
Phe ¹⁰⁵	Leu ¹¹³	Smaller, remains hydrophobic
Lys ¹¹⁹	Thr ¹²⁷	Loss of positive charge
Ser ¹³⁷	Trp ¹⁴⁵	Polar residue changed to bulky hydrophobic
Arg ¹³⁸	Lys ¹⁴⁶	Conservative change
Ile ³⁰⁴	Val ³⁰⁶	Conservative change
Ala ³¹³	Ser ³¹⁵	Becomes more polar
Val ⁴⁰⁴	Ile ⁴⁰⁴	Conservative change
Val ⁵¹⁰	Thr ⁵¹²	Becomes more polar

^a None of these changed residues are part of the active site (Fig. 1A).

explanation for the relative resistance of the ckCYP51 to inhibition by fluconazole and voriconazole. It is possible that subtle differences in the active sites of the two enzymes do contribute significantly to fluconazole resistance in *C. krusei*. For example, F105 is predicted to be within 12 Å of the active site of caCYP51 and the F105L substitution is associated with fluconazole resistance in *C. albicans* (12). Interestingly, the F105L substitution is also present in the ckCYP51 (13), suggesting that this substitution may contribute to fluconazole resistance in *C. krusei*.

Analysis of other mutations in caCYP51 that are associated with azole resistance in *C. albicans* indicates that many of the amino acid substitutions are located in regions of the protein that are predicted to be outside of the substrate binding site (13, 20). These substitutions may change the conformation of the binding site and/or limit access to it. The use of site-directed mutagenesis to change the key amino acids that differ between caCYP51 and ckCYP51 will enable us to refine the three-dimensional models of both enzymes, so that the relative resistance of ckCYP51 to azoles can be explained. These investigations are currently in progress.

ACKNOWLEDGMENTS

We thank Quynh T. Phan and Angela Sanchez for technical assistance.

This work was supported in part by an unrestricted grant from Pfizer, Inc. S. G. Filler was supported by the Burroughs-Wellcome Fund New Investigator Award in Molecular Pathogenic Mycology.

REFERENCES

- Abbas, J., G. P. Bodey, H. A. Hanna, M. Mardani, E. Girgawy, D. Abi-Said, E. Whimbey, R. Hachem, and I. Raad. 2000. *Candida krusei* fungemia. An escalating serious infection in immunocompromised patients. *Arch. Intern. Med.* **160**:2659–2664.
- Abola, E. E., J. L. Sussman, J. Prilusky, and N. O. Manning. 1997. Protein Data Bank archives of three-dimensional macromolecular structures. *Methods Enzymol.* **277**:556–571.
- Agatep, R., R. Kirkpatrick, D. Parchaliuk, R. Woods, and R. Gietz. 1998. Transformation of *Saccharomyces cerevisiae* by the lithium acetate/single-stranded carrier DNA/polyethylen glycol (LiAc/ss-DNA/PEG) protocol. *Tech. Tips Online* [Online.] <http://tto.trends.com>.
- Burgener-Kairuz, P., J. P. Zuber, P. Jaunin, T. G. Buchman, J. Bille, and M. Rossier. 1994. Rapid detection and identification of *Candida albicans* and *Torulopsis (Candida) glabrata* in clinical specimens by species-specific nested PCR amplification of a cytochrome P-450 lanosterol- α -demethylase (L1A1) gene fragment. *J. Clin. Microbiol.* **32**:1902–1907.
- Espinell-Ingroff, A., K. Boyle, and D. J. Sheehan. 2001. In vitro antifungal activities of voriconazole and reference agents as determined by NCCLS methods: review of the literature. *Mycopathologia* **150**:101–115.
- Goldman, M., J. C. Pottage, Jr., and D. C. Weaver. 1993. *Candida krusei* fungemia. Report of 4 cases and review of the literature. *Medicine (Baltimore)* **72**:143–150.
- Iwen, P. C., D. M. Kelly, E. C. Reed, and S. H. Hinrichs. 1995. Invasive infection due to *Candida krusei* in immunocompromised patients not treated with fluconazole. *Clin. Infect. Dis.* **20**:342–347.
- Ji, H., W. Zhang, Y. Zhou, M. Zhang, J. Zhu, Y. Song, and J. Lu. 2000. A three-dimensional model of lanosterol 14 α -demethylase of *Candida albicans* and its interaction with azole antifungals. *J. Med. Chem.* **43**:2493–2505.
- Katiyar, S. K., and T. D. Edlind. 2001. Identification and expression of multidrug resistance-related ABC transporter genes in *Candida krusei*. *Med. Mycol.* **39**:109–116.
- Lamb, D. C., D. E. Kelly, T. C. White, and S. L. Kelly. 2000. The R467K amino acid substitution in *Candida albicans* sterol 14 α -demethylase causes drug resistance through reduced affinity. *Antimicrob. Agents Chemother.* **44**:63–67.
- Laskowski, R. A., M. W. McArthur, D. S. Moss, and J. M. Thornton. 1993. PROCHECK: a program to check the stereochemical quality of protein structures. *J. Appl. Crystallogr.* **26**:283–291.
- Loffler, J., S. L. Kelly, H. Hebart, U. Schumacher, C. Lass-Flörl, and H. Einsele. 1997. Molecular analysis of cyp51 from fluconazole-resistant *Candida albicans* strains. *FEMS Microbiol. Lett.* **151**:263–268.

13. Marichal, P., L. Koymans, S. Willemsens, D. Bellens, P. Verhasselt, W. Luyten, M. Borgers, F. C. Ramaekers, F. C. Odds, and H. V. Bossche. 1999. Contribution of mutations in the cytochrome P450 14 α -demethylase (Erg11p, Cyp51p) to azole resistance in *Candida albicans*. *Microbiology* **145**:2701–2713.
14. National Committee for Clinical Laboratory Standards. 1997. Reference method for broth dilution antifungal susceptibility testing of yeasts: approved standard. NCCLS document M27-A. National Committee for Clinical Laboratory Standards, Wayne, Pa.
15. Nguyen, M. H., and C. Y. Yu. 1998. Voriconazole against fluconazole-susceptible and resistant candida isolates: in-vitro efficacy compared with that of itraconazole and ketoconazole. *J. Antimicrob. Chemother.* **42**:253–256.
16. Ochman, H., A. S. Gerber, and D. L. Hartl. 1988. Genetic applications of an inverse polymerase chain reaction. *Genetics* **120**:621–623.
17. Orozco, A. S., L. M. Higginbotham, C. A. Hitchcock, T. Parkinson, D. Falconer, A. S. Ibrahim, M. A. Ghannoum, and S. G. Filler. 1998. Mechanism of fluconazole resistance in *Candida krusei*. *Antimicrob. Agents Chemother.* **42**:2645–2649.
18. Pesole, G., M. Lotti, L. Alberghina, and C. Saccone. 1995. Evolutionary origin of nonuniversal CUG^{Ser} codon in some *Candida* species as inferred from a molecular phylogeny. *Genetics* **141**:903–907.
19. Podust, L. M., T. L. Poulos, and M. R. Waterman. 2001. Crystal structure of cytochrome P450 14 α -sterol demethylase (CYP51) from *Mycobacterium tuberculosis* in complex with azole inhibitors. *Proc. Natl. Acad. Sci. USA* **98**:3068–3073.
20. Podust, L. M., J. Stojan, T. L. Poulos, and M. R. Waterman. 2001. Substrate recognition sites in 14 α -sterol demethylase from comparative analysis of amino acid sequences and X-ray structure of *Mycobacterium tuberculosis* CYP51. *J. Inorg. Biochem.* **87**:227–235.
21. Sali, A., and T. L. Blundell. 1993. Comparative protein modelling by satisfaction of spatial restraints. *J. Mol. Biol.* **234**:779–815.
22. Sanglard, D., F. Ischer, L. Koymans, and J. Bille. 1998. Amino acid substitutions in the cytochrome P-450 lanosterol 14 α -demethylase (CYP51A1) from azole-resistant *Candida albicans* clinical isolates contribute to resistance to azole antifungal agents. *Antimicrob. Agents Chemother.* **42**:241–253.
23. Sorkhoh, N. A., M. A. Ghannoum, A. S. Ibrahim, R. J. Stretton, and S. S. Radwan. 1991. Growth of *Candida albicans* in the presence of hydrocarbons: a correlation between sterol concentration and hydrocarbon uptake. *Appl. Microbiol. Biotechnol.* **34**:509–512.
24. Sussman, J. L., D. Lin, J. Jiang, N. O. Manning, J. Prilusky, O. Ritter, and E. E. Abola. 1998. Protein Data Bank (PDB): database of three-dimensional structural information of biological macromolecules. *Acta Crystallogr. D Biol. Crystallogr.* **54**:1078–1084.
25. Talele, T. T., S. S. Kulkarni, and V. M. Kulkarni. 1999. Development of pharmacophore alignment models as input for comparative molecular field analysis of a diverse set of azole antifungal agents. *J. Chem. Infect. Comput. Sci.* **39**:958–966.
26. Talele, T. T., and V. M. Kulkarni. 1999. Three-dimensional quantitative structure-activity relationship (QSAR) and receptor mapping of cytochrome P-450(14 α DM) inhibiting azole antifungal agents. *J. Chem. Infect. Comput. Sci.* **39**:204–210.
27. Talibi, D., and M. Raymond. 1999. Isolation of a putative *Candida albicans* transcriptional regulator involved in pleiotropic drug resistance by functional complementation of a *pdrl pdr3* mutation in *Saccharomyces cerevisiae*. *J. Bacteriol.* **181**:231–240.
28. Triglia, T., M. G. Peterson, and D. J. Kemp. 1988. A procedure for in vitro amplification of DNA segments that lie outside the boundaries of known sequences. *Nucleic Acids Res.* **16**:8186.
29. Venkateswarlu, K., D. W. Denning, N. J. Manning, and S. L. Kelly. 1996. Reduced accumulation of drug in *Candida krusei* accounts for itraconazole resistance. *Antimicrob. Agents Chemother.* **40**:2443–2446.